A&A 454, 295–299 (2006)
DOI: 10.1051/0004-6361:20052989

Astronomy & Astrophysics

The RS CVn binary HK Lacertae: long-term photometry from Sonneberg sky-patrol plates⋆

H.-E. Fröhlich[1], P. Kroll[2], and K. G. Strassmeier[1]

[1] Astrophysikalisches Institut Potsdam (AIP), An der Sternwarte 16, 14482 Potsdam, Germany
e-mail: [hefroehlich;kstrassmeier]@aip.de
[2] Sternwarte Sonneberg, Sternwartestr. 32, 96515 Sonneberg, Germany
e-mail: pk@4pisysteme.de

Received 4 March 2005 / Accepted 14 March 2006

ABSTRACT

Long-term photographic photometry of the active long-period RS CVn binary HK Lac (HD 209813) was obtained from more than 2000 Sonneberg Sky-Patrol plates taken between 1956 and 1996. We achieve an internal accuracy of $0\overset{m}{.}07$. The correspondence with contemporaneous high-precision photoelectric photometry from automatic telescopes is striking and successfully demonstrates the feasibility of our approach. Based on a Bayesian time series analysis, we improve the previously published cycle period to 13.37 ± 0.08 years, and present evidence of an additional period of 9.48 ± 0.13 years. This establishes the multi-periodicity of dynamo action in these overactive stars as compared to the Sun. The already known 6.7-years cycle turns out to be an overtone of the dominating 13.4-years cycle. Our long-term photographic photometry even allowed the detection of the star's mean rotational period of 24.35 days.

Key words. stars: activity – stars: individual: HK Lacertae – stars: late-type – stars: rotation – stars: starspots

1. Introduction

Stellar dynamo theory is reaching a level of sophistication that it is on the verge of being successfully confronted with observations, i.e., with measured properties of magnetically-driven stellar activity (for an overview cf. Rosner 2000; Rüdiger & Hollerbach 2004). One of the dynamo observables is the time series of stellar activity, especially cycle lengths and their variations. Long-term studies (Baliunas et al. 1995) of stellar activity rely mostly on the chromospheric Ca II emission, the so-called S-index, as monitored e.g. at the Mount Wilson Observatory. For very active stars the varying spottedness leads even to a measurably long-term variation in the mean photospheric brightness (Messina et al. 2001; Messina & Guinan 2002). We adopt here the view that these light variations are solely magnetic in origin (Solanki 2002).

The target HK Lac has been chosen because of its long photoelectric timeseries. Its variability was discovered by Blanco & Catalano (1968). Since then it has been monitored regularly (Oláh et al. 1997) and is now considered a long-period RS CVn binary (Hall 1976; Strassmeier et al. 1993). For further details see Oláh et al. (1997) and Oláh & Strassmeier (2002).

By inspecting archival photographic material and combining it with photoelectric data, Phillips & Hartmann (1978) detected a 50−60 year cycle for BY Dra and CC Eri. Because the photometric precision is low, $\lesssim$0.1 mag, follow-up research has concentrated on photoelectric measurements with dedicated automatic photoelectric telescopes (APTs) (cf. Strassmeier et al. 1997a). Focusing on ten well-studied rapidly-rotating active stars, mostly components of RS CVn-type binary systems, the APTs revealed the existence of multi-periodic photospheric cycles in these stars (Oláh et al. 2000). This resembles the solar behavior where, along with the well-known eleven year photometric cycle, at least one longer cycle, the Gleissberg cycle, exists. In the case of the giant star HK Lac, the photoelectric time-series extends over 35 years (Oláh & Strassmeier 2002).

For some stars, the data reveal only long-term trends, probably indicating cycles with very long periods. One example is the solar analog EK Draconis (Fröhlich et al. 2002). Moreover, many cycle lengths are often suspiciously near the total length of the time-base being monitored. Obviously, the search for decade-long activity cycles is hampered by the non-availability of long-term photoelectric data.

The only approach to increasing the time coverage considerably is to exploit plate archives (cf. Kroll et al. 2001), as has been demonstrated by the work of Phillips & Hartmann (1978), Hartmann et al. (1979), Hartmann et al. (1981), Bondar' (1995), Alekseev & Bondar' (1998), Fröhlich et al. (2002), and Innis et al. (2004). Even though the photometric accuracy of a photographic brightness measure is low, averaging over dozens of measures nevertheless gives an accurate long-term *mean* light curve. Even long-term photoelectric measurements must be averaged to suppress the rotationally-induced short-term brightness variation, which is often comparable to the error of photographic photometry. Especially interesting in this respect is the Sonneberg Observatory Sky Patrol (Bräuer & Richter 1994; Kroll et al. 1999; Bräuer et al. 1999). It started in the mid-fifties and has used the same equipment since then. In 1997 the plates were superseded by sheet films, though.

⋆ Table 1 is only available in electronic form at the CDS via anonymous ftp to cdsarc.u-strasbg.fr (130.79.128.5) or via http://cdsweb.u-strasbg.fr/cgi-bin/qcat?J/A+A/454/295

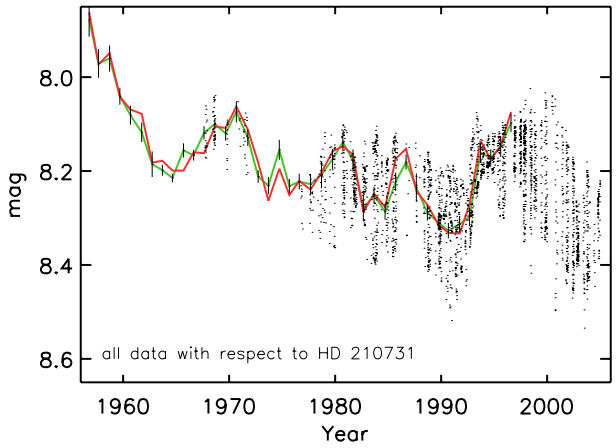

Fig. 1. B^{T} light curve of HK Lac. The green (light grey) line connects the seasonal averages, the red (darker grey) one shows the median values. Bars indicate the standard error of the mean. Over-plotted are the photoelectric measurements as dots (see text). The correspondence between the two data sets in the overlap region is striking.

In this paper, we demonstrate the feasibility of such an approach by performing photographic photometry of the active binary system HK Lac and comparing it with photoelectric data that has been gathered since 1967 (Oláh et al. 1997).

2. Observations

2.1. Sonneberg Sky Patrol

Since the mid-fifties a modernized photographic Sky-Patrol program with 14 short-focus 55/250-cameras has monitored the sky north of $\delta \gtrsim -20°$ at Sonneberg Observatory (Bräuer & Richter 1994). This wide-field Sky Patrol with $26° \times 26°$ FOV has aimed at long-term studies of variable stars. It was operated simultaneously in two band-passes, a (blue) photographic region with a limiting magnitude of 14^{m} and a (red-yellow) photo-visual region down to 13^{m}. From 1956 onwards, more than 2000 plates in total of the three sky fields (with center positions: RA = 21^{h}, 22^{h}, and 23^{h}, $\delta = 40°$) containing HK Lac ($22^{\mathrm{h}}5^{\mathrm{m}}$, $47°14'$) were taken. The digitized plate images (16 bit depth) obtained with fast scanners have a spatial resolution of 21 μm, corresponding to 17.6″/pixel.

2.2. Photoelectric data

Photoelectric data are being obtained continuously since the discovery of the light variability of HK Lac in 1967. A recent summary of the available data was given by Oláh et al. (1997). The bulk of the data came from the APTs at Fairborn Observatory in southern Arizona (Boyd et al. 1984). Figure 1 shows a total of 2500 photoelectric B-band data. The data from 1995 on were obtained with the Vienna-T7-APT (Strassmeier et al. 1997b), now jointly operated by the AIP and the University of Vienna, and taken in the Johnson-Cousins VI system and converted to $B \approx B^{\mathrm{T}}$ with the help of Eq. (1) and $(B-V)^{\mathrm{T}}_{\mathrm{HKLac}} = 1.227$.

3. Long-term photographic photometry

In order to take all sorts of non-homogeneity effects into account, one can only rely on the presumed constancy of comparison stars in the neighborhood of the program star. The B^{T} and V^{T} magnitudes of these putatively constant comparison stars are taken from the Tycho-2 catalog (Høg et al. 2000a,b). The photometric system differs slightly from Johnson's UBV. For main-sequence stars the approximation

$$V = V^{\mathrm{T}} - 0.090\,(B-V)^{\mathrm{T}}, (B-V) = 0.850\,(B-V)^{\mathrm{T}} \quad (1)$$

seems to hold (Perryman 1997).

3.1. Outline of the method

A single brightness estimate on a scanned Sky-Patrol plate is accurate to 0.07–0.1 mag (Vogt & Kroll 1999). By averaging over N estimates, one can at best hope to reduce the photometric error according to the $N^{-1/2}$-law (in the absence of systematic errors). Rotationally induced short-term brightness variations are considered here as an additional random noise.

We adopted a semi-automatic approach. The images were inspected using MIDAS routines (cf. ESO's MIDAS site `http://www.eso.org/projects/esomidas/`). The crude positions of five stars, including HK Lac, were determined by eye and saved by clicking on the appropriate stellar images. This established a local coordinate system. The positions of further comparison stars with known sky coordinates were than computed automatically.

3.2. Comparison stars

A total of 17 standard stars were used. The stars span a brightness range from $6\overset{\mathrm{m}}{.}2 \le B^{\mathrm{T}} \le 9\overset{\mathrm{m}}{.}3$, covering HK Lac's mean magnitude of $B^{\mathrm{T}} \approx 8\overset{\mathrm{m}}{.}3$. The situation with regard to color is somewhat worse. Only one comparison star, a K2 star, is as red as HK Lac, while all the other stars are bluer. Unfortunately, the reddest star is also the weakest, thereby introducing an artificial correlation in the B^{T} vs. $(B-V)^{\mathrm{T}}$ plane for the fiducial stars. Except for another K star (K0), all the other (15) comparison stars belong to spectral types B, A, and F.

We varied the set of comparison stars throughout the measurement procedure, including some new stars and excluding some others. The shape of the resulting light curve proved rather robust though, but sometimes we had to apply some zero point adjustment to bring the photographic and the photoelectric light curve to coincidence.

3.3. Parameter fitting

All plates are photometrically un-calibrated. Therefore, some kind of interpolation from plate to plate must be involved. In order to get a proxy for a stellar magnitude within each plate's photometric system, one first has to assume a characteristic curve to convert photographic densities to pseudo intensities. These pseudo magnitudes are assumed to depend monotonically on the real magnitudes.

As in Fröhlich et al. (2002) we neglected any non-linearity in the characteristic curve and fixed the gradation to $\gamma = 1$ (Kroll & Neugebauer 1993).

These intensities are estimates with respect to the local sky background. The mode of the frequency distribution of intensity in a $50\,\mathrm{px} \times 50\,\mathrm{px}$ field around each star was assigned an arbitrary unit value. After background subtraction and integration over all pixels within the circular aperture of a five-pixel radius, we get a pseudo magnitude. To convert pseudo magnitudes into real plate magnitudes, $\mathrm{mag_i}$, a cubic fitting procedure was applied.

In order to tie the plate magnitudes into the Tycho-2 photometric system, one has to apply color corrections. Here we restrict ourselves to the ansatz of Eq. (2), where the coefficients in the color equation depend linearly on time, which is a rather conservative approach that may introduce at most spurious trends but never periods:

$$B_i^{\mathrm{T}} = \mathrm{mag}_{\mathrm{i}}^{\mathrm{plate}} + (p_1 + p_2 \cdot (t_{\mathrm{a}} - 1975)) \cdot (B-V)_i^{\mathrm{T}} + (p_3 + p_4 \cdot (t_{\mathrm{a}} - 1975)) \cdot \left((B-V)_i^{\mathrm{T}}\right)^2 + \mathrm{const.}, \quad (2)$$

where t_{a} denotes the year and const. merely means a nuisance parameter for each plate. Variables labeled with a superscript "T" refer to Tycho-2 values.

In the end we found that any time-dependence only marginally improved the fit. Therefore, the parameters p_2 and p_4 were omitted. Because we used three kinds of plates, viz. 980 photographic (pg), 816 photo-visual (pv), and 241 panchromatic (p) plates, there are altogether six free parameters to be solved for by minimizing the mean residual deviation. The mode of the mean photometric accuracy turned out to be $0\overset{\mathrm{m}}{.}07$. This modal value does not depend on the Sky-Patrol field chosen. But in the RA 21^{h}-field and in the 23^{h}-field, where the target star is more outside the center than in the 22^{h}-field, the distribution function of the photometric accuracy is – as anticipated – significantly skewed towards larger photometric errors.

3.4. Internal accuracy

One plate, arbitrarily chosen, has been scanned an additional 16 times, with four scanners and in each case with four orientations. This allowed us to crudely estimate an internal error of $0\overset{\mathrm{m}}{.}05$.

4. Results

4.1. The 48-year long light curve of HK Lac

Figure 1 shows the photographic light curve of HK Lac from the Sky-Patrol plates from 1956 through 1996. Its differential magnitudes were converted to a B^{T} brightness with the help of HD 210731. (All the photographic data is in Table 1, available only electronically.) Also shown are the photoelectric B data (cf. Oláh et al. 1997) whenever available and supplemented by further unpublished APT data (dots). Photoelectric V data were converted to B magnitudes by simply using the long-term mean $B-V$. The striking correspondence between the photographic seasonal averages and the individual photoelectric measurements is intriguing and proves the feasibility of our photographic approach, even for target stars as faint as 8th magnitude. One has to keep in mind, though, that changing the set of comparison stars could lead to small vertical shifts between the two light curves.

A more severe effect is that some comparison stars may exhibit a significant long-term trend themselves (cf. Vogt et al. 2004). With the color-Eq. (2) alone, it seems impossible to suppress such long-term trends. Deviating from the best set of parameters constrained by least-squares minimization, p_i, simply does not remove this. In this respect, the strong decline at the beginning of the data is possibly suspicious.

Nevertheless, the star was significantly brighter in the past than it is today. A conservative value is $0\overset{\mathrm{m}}{.}20-0\overset{\mathrm{m}}{.}25$ brighter than in 2000. In 1956, the star was $\approx 7\overset{\mathrm{m}}{.}95$, while the mean brightness in 2000 was $8\overset{\mathrm{m}}{.}2$ (on the B^{T} scale). Such long-term changes are usually attributed to the overall degree of spot coverage or, in case the star is known to have a polar spot from Doppler imaging, also to the changing size of its polar spot. Weber et al. (2000) and Weber (2004) presented the first Doppler images of HK Lac and found no polar spot but several large spots at medium latitudes. Oláh et al. (1997) computed unspotted BV magnitudes of $-0\overset{\mathrm{m}}{.}30$ and $-0\overset{\mathrm{m}}{.}74$, respectively (with respect to HD 210731), from a relation between amplitude and the overall brightness of the star. Assuming roughly $B \approx B^{\mathrm{T}}$, the predicted unspotted magnitude in Fig. 1 would be at $\approx 7\overset{\mathrm{m}}{.}8$, still brighter than the currently brightest observation in 1956.

Table 2. The list of hypotheses H_i being considered. Given are besides the number of parameters used, $p_{\max}$, the average gain in mean likelihood per data point (in percent) and the value h_i of each hypothesis, both with regard to the zero hypothesis.

Hypothesis	$p_{\max}$	gain	h_i/h_0
H_0: null hypothesis	2	0	1
H_1: one fundamental mode (f.m.)	5	9.8 p.c.	2×10^{194}
H_2: one f.m. + one overtone	7	11.4 p.c.	2×10^{223}
H_3: one f.m. + two overtones	9	11.8 p.c.	1×10^{231}
H_4: two f.m.	8	12.2 p.c.	4×10^{237}
H_5: H_3 + an additional f.m.	12	14.2 p.c.	3×10^{275}

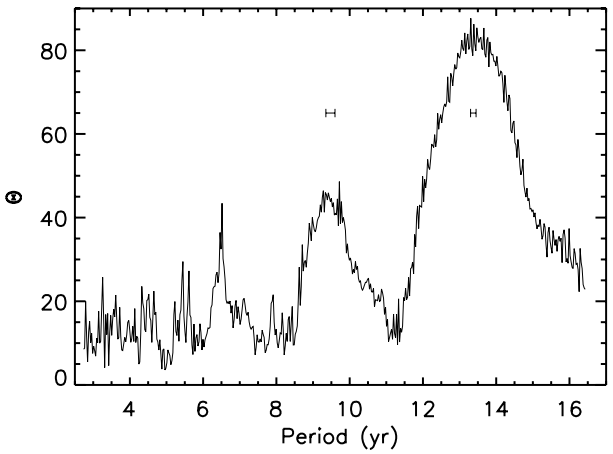

Fig. 2. Periodogram of HK Lac from the combined data, photographic as well as photoelectric. There is an indication of a further 9.5-year cycle besides the already suggested cycles of 6.8 and 13.0 years from photoelectric photometry alone (Oláh et al. 2000). The two bars mark Bayesian 90 percent confidence regions around periods of 9.48, and 13.37 years (mean values).

4.2. Search for activity cycles

After removing a linear trend, the period range 1000 days to 6000 days has been scanned by an analysis of variance (AoV) period search (cf. Schwarzenberg-Czerny 1989). The periodogram is shown in Fig. 2. Three bumps are easily discernable, at 6.7, 9.5, and 13.4 years. A cycle length around 10 years is not mentioned in the literature. Maybe, the shortest period is just an overtone of the longest one. How significant are these cycles? Because the period of the longest one is not short as compared with the 48-year time base, a Bayesian approach is indicated, e.g. Bretthorst (1988). In order to allow for a deviation from a sinusoidal behavior overtones are included. A set of hypotheses, H_i, is evaluated (cf. Table 2). Because the probability of a hypothesis, h_i, is the *mean* likelihood over the parameter space, one has to prescribe the parameter ranges beforehand. All probabilities are with regard to the null hypothesis, i.e., no periodicity at all.

The most general fitting function (hypothesis H_5) is as follows. The null hypothesis H_0 allows for an off-set and a linear trend in time t.

$$\begin{aligned} f_0(t_i) \;=\; & p_1 + p_2 \cdot t_i \\ & + p_3 \cdot \cos(\; p_4 \cdot t_i + p_5) + p_6 \cdot \cos(2p_4 \cdot t_i + p_7) \\ & + p_8 \cdot \cos(3p_4 \cdot t_i + p_9) + p_{10} \cdot \cos(p_{11} \cdot t_i + p_{12}). \end{aligned} \quad (3)$$

The likelihood for a given set of n data points $d_i(t_i)$ at some location $p_1 \ldots p_{\max}$ in parameter space is

$$\Lambda(\sigma, p_1 \ldots p_{\max}) \;\propto\; \frac{1}{\sigma^n} \exp\left(-\frac{1}{2\sigma^2} \sum_{i=1}^{n} (d_i - f_0(t_i))^2\right), \quad (4)$$

where σ denotes the Gaussian standard deviation and "max" $\leq$12 the maximal number of parameters belonging to a certain hypothesis.

The mean likelihood, which measures the strength of a hypothesis, is then found by integrating over parameter space:

$$\overline{\Lambda} = \int w_1 \cdots w_{\max} \cdot \Lambda(\sigma, p_1 \ldots p_{\max}) \, \frac{\mathrm{d}\sigma}{\sigma} \, \mathrm{d}p_1 \cdots \mathrm{d}p_{\max}. \quad (5)$$

The *constant* priors w_i are subject to the normalization constraint

$$\int w_1 \cdots w_{\max} \, \mathrm{d}p_1 \cdots \mathrm{d}p_{\max} = 1. \quad (6)$$

It is important that the standard deviation σ, comprising the photometric error, as well as any small-scale fluctuations, is considered for feasibility reasons as an unknown parameter, too. The integration over σ has been performed using the Jeffreys σ^{-1} prior. It results in an expression that can be *analytically* integrated further (Köppen & Fröhlich 1997). Only the integration over the unknown phases p_5, p_7, p_9, p_{12} and over the two frequencies p_4 and p_{11}, respectively, have to be performed numerically. With σ being a further unknown parameter the Bayesian approach proves tractable!

Amplitudes are integrated analytically from $-\infty$ to ∞, and phases numerically from 0 to π. Speaking exactly, the amplitudes should be integrated over some finite range and fixed a priori, say -0.1 mag to $+0.1$ mag. For the sake of computability the finite integrals are substituted by the analytical ones extending over infinite ranges. The difference is, in any case, small because large amplitudes are obviously absent and cannot contribute.

Because it is the ratio h_i/h_0 of mean likelihoods that makes sense, only the frequency priors w_4, w_{11}, the amplitude prior $w_{10} = 5$, and the phase prior $w_{12} = \pi^{-1}$ must be specified. Generally we are looking for periods P between 8 and 16 years. In the case of two fundamental modes, i.e., hypothesis H_5, the frequency space is split (at least in theory) according to $8 \leq P_{\mathrm{short}} = 2\pi/(365.2425 p_{11}) < P_{\mathrm{long}} = 2\pi/(365.2425 p_4) \leq 16$ years. (Actually the two intervals $9 \leq P_{\mathrm{short}} < 10$ years and $13 < P_{\mathrm{long}} \leq 14$ years have been scanned.) The high frequency region $P \leq 8$ years is exploited only by the two overtones of the longest cycle. The numerical integration over a six-dimensional sub space was performed with the aid of a 128-nodes PC cluster.

Introducing a second fundamental mode in addition to the 13.4 years cycle with two overtones (H_3) results in a gain in the goodness of fit by a stunning factor of 3×10^{44}! Hence it definitely makes sense to consider at least two cycles as present in the data. This tremendous gain in mean likelihood is owing to the large number of data points, $n = 4766$. An average gain per data point of one per cent raises the probability already by a factor $1.01^{4766} \approx 4 \times 10^{20}$.

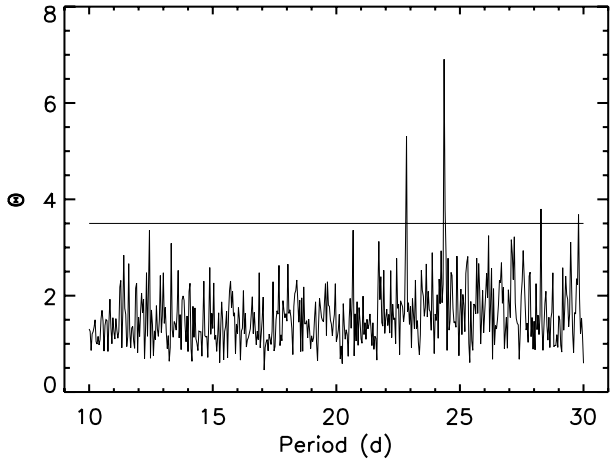

Fig. 3. The detection of HK Lac's rotational period from long-term photographic plates. Five hundred trial periods were searched. The period is in days. The most prominent peak is the star's rotational period of 24.35 days. The nearby 22.8-day peak is due to a sampling artefact. Multiples of these periods, not shown here, exist as well. The one percent level of significance, $\overline{\Theta}_{0.01} = 3.5$, is marked by the horizontal line.

Note that there is no indication of a third cycle within the range of $8 \leq P \leq 16$ years. From the *marginal* distributions of the two frequencies p_4 and p_{11}, one gets the expectation values of the periods, exactly speaking $1/\langle 1/P \rangle$, as well as estimates of the 90 percent confidence intervals: 9.48 ± 0.13 and 13.37 ± 0.08 years. Since the amplitudes have by necessity been regarded as nuisance parameters, only the modal values can be given: 0.054 mag (13.4 years cycle), 0.034 mag (9.5 years cycle), 0.026 mag (13.4/2 years cycle), and 0.015 mag (13.4/3 years cycle).

The two periods found are most probably not sampling artefacts. We replaced one thousand times the measured magnitude values at the 4766 time instants by random numbers drawn from a Gaussian distribution and searched the artificial "data" sets in each case for one fundamental mode. (The scale of the noise does not matter, for it is assumed that nothing is known about σ.) No preferred periods are indicated. Moreover, only in 12 percent or so of all cases did the null hypothesis have to be rejected because $h_1 \geq h_0$.

4.3. Search for the rotational period of HK Lac

After pre-whitening the data with a 6th-order polynomial, the period range 10 days to 80 days was again scanned with the AoV algorithm. The periodogram ($10\,\mathrm{d} \leq P \leq 30\,\mathrm{d}$) is shown in Fig. 3. The most prominent peak is HK Lac's average photometric period of 24.35 days. The other peaks, significant at the one percent level, are most probably sampling artefacts due to the gaps between the observing seasons and the interplay of the synodic month with the dominating fundamental mode.

In the case of Gaussian white noise, the test statistic Θ should be distributed according to Fisher's F distribution with the expectation value being nearly exactly one (cf. Schwarzenberg-Czerny 1989). The latter obviously does not hold here.

In order to assign a significance to the 24.35-day period, we applied a bootstrap method. The period interval 10–30 days was covered with 500 trial periods. Then, 2000 randomly reshufflings of the 500 Θ's resulted in 2000 distribution functions, i.e., 2000 values for the one-percent level of significance.

The resulting signal for the 24.35-day period is clearly above the latter's mean value of $\overline{\Theta}_{0.01} = 3.5$.

Due to the finite time span of 40 years, the half-line width at $P = 24.35\,\mathrm{d}$ is $\approx$0.04 days. The location of the line center, the period itself, is of course better defined. In view of the high noise level, it would make no sense to apply a more sophisticated period searching algorithm like a wavelet analysis.

5. Conclusions

1. The feasibility of our photographic approach to establishing decadal light variation in the seasonal averages of very active 8th-mag stars has been demonstrated.
2. The putative 13.0 and 6.8 year periods (Oláh et al. 2000) (but cf. Oláh & Strassmeier 2002) are confirmed. The fundamental period has now been revised to 13.37 ± 0.08 years. The short period is a mere overtone of that cycle. Within the set of hypotheses, $H_0 \ldots H_5$, the hypothesis H_5, considering two fundamental modes, is assigned the highest probability. This second cycle has a period of 9.48 ± 0.13 years.
3. The AoV algorithm suggests a rotational period of 24.35 days in the photographic data, possibly indicating that the active longitude persisted for decades.

Acknowledgements. The authors wish to thank the anonymous referee for helpful suggestions. This work would not have been possible without the generous support by our colleagues at the Sonneberg Observatory, especially Klaus Löchel and Hans-Jürgen Bräuer. Part of this work was supported by the German *Deutsche Forschungsgemeinschaft, DFG* project STR645/1 and by the Company 4pi Systeme GmbH. The APTs in Arizona are jointly operated by the University of Vienna and the AIP.

References

Alekseev, I. Y., & Bondar', N. I. 1998, Astronomy Reports, 42, 655
Baliunas, S. L., Donahue, R. A., Soon, W. H., et al. 1995, ApJ, 438, 269
Blanco, C., & Catalano, S. 1968, IBVS, 253, 2
Bondar', N. I. 1995, A&AS, 111, 259
Boyd, L. J., Genet, R. M., & Hall, D. S. 1984, IAPPP Comm., 15, 20
Bräuer, H.-J., & Richter, G. A. 1994, in Astronomy from Wide-Field Imaging, ed. H. T. MacGillivray, et al., IAU Symp., 161, 43
Bräuer, H., Häusele, I., Löchel, K., & Polko, N. 1999, Acta Historica Astronomiae, 6, 70
Bretthorst, G.L. 1988, Bayesian Spectrum Analysis and Parameter Estimation (New York: Springer)
Fröhlich, H.-E., Tschäpe, R., Rüdiger, G., & Strassmeier, K. G. 2002, A&A, 391, 659
Hall, D. S. 1976, in Multiple Periodic Variable Stars, ed. W. S. Fitch, IAU Colloq., 29, 287
Hartmann, L., Londono, C., & Phillips, M. J. 1979, ApJ, 229, 183
Hartmann, L., Dussault, M., Noah, P. V., Klimke, A., & Bopp, B. W. 1981, ApJ, 249, 662
Høg, E., Fabricius, C., Makarov, V. V., et al. 2000a, A&A, 357, 367
Høg, E., Fabricius, C., Makarov, V. V., et al. 2000b, A&A, 355, L27
Innis, J. L., Borisova, A. P., Coates, D. W., & Tsvetkov, M. K. 2004, MNRAS, 355, 591
Köppen, J., & Fröhlich, H.-E. 1997, A&A, 325, 961
Kroll, P., & Neugebauer, P. 1993, A&A, 273, 341
Kroll, P., La Dous, C., & Bräuer, H., 1999, Treasure-Hunting in Astronomical Plate Archives, Acta Historica Astronomiae, Vol. 6 (Verlag Harri Deutsch, Thun u. Frankfurt a. Main)
Kroll, P., Vogt, N., Bräuer, H.-J., & Splittgerber, E. 2001, in MPA/ESO/MPE Workshop, Mining the Sky, ed. A. J. Banday, S. Zaroubi, & M. Bartelmann, 511
Messina, S., & Guinan, E. F. 2002, A&A, 393, 225
Messina, S., Rodonò, M., & Guinan, E. F. 2001, A&A, 366, 215
Oláh, K., & Strassmeier, K. G. 2002, AN, 323, 361
Oláh, K., Kővári, Z., Bartus, J., et al. 1997, A&A, 321, 811
Oláh, K., Kolláth, Z., & Strassmeier, K. G. 2000, A&A, 356, 643
Perryman, M. A. C. 1997, ESA SP-1200, 120
Phillips, M. J., & Hartmann, L. 1978, ApJ, 224, 182
Rosner, R. 2000, in Philos. Trans. R. Soc. London, Ser. A, Magnetic activity in stars, discs and quasars, 358, 689
Rüdiger, G., & Hollerbach, R. 2004, The Magnetic Universe: Geophysical and Astrophysical Dynamo Theory (Weinheim: Wiley-VCH)
Schwarzenberg-Czerny, A. 1989, MNRAS, 241, 153
Solanki, S. K. 2002, AN, 323, 165
Strassmeier, K. G., Hall, D. S., Fekel, F. C., & Scheck, M. 1993, A&AS, 100, 173
Strassmeier, K. G., Bartus, J., Cutispoto, G., & Rodonò, M. 1997a, A&AS, 125, 11
Strassmeier, K. G., Boyd, L. J., Epand, D. H., & Granzer, T. 1997b, PASP, 109, 697
Vogt, N., & Kroll, P. 1999, Acta Historica Astronomiae, 6, 210
Vogt, N., Kroll, P., & Splittgerber, E. 2004, A&A, 428, 925
Weber, M. 2004, Ph.D. Thesis, Univ. Potsdam
Weber, M., Strassmeier, K. G., & Washüttl, A. 2000, in Stellar Clusters and Associations: Convection, Rotation, and Dynamos, ed. R. Pallavicini, G. Micela, & S. Sciortino, ASP Conf. Ser., 198, 495